ELSEVIER

Interaction of two opposite conical curved wall jets

M. A. Jarrah, T. K. Aldoss, and A. M. Al-Sarkhi
Jordan University of Science and Technology, Department of Mechanical Engineering, Irbid, Jordan

An experimental investigation of a conical flow formed by the interaction of two asymmetric turbulent curved wall jets past a circular cone is presented. Measurements were made of velocity and turbulence intensity profiles of the two jets in the wall jet, the interaction, and the merged jet regions. The location of the interaction region of the two opposing curved wall jets and the flow direction of the merged jet were found to depend primarily on the ratio of the slot exit velocities of the two jets. The mean velocity and streamwise turbulence intensity profiles of the merged jet were similar to those in a turbulent free jet. Regardless of jet-exit velocity ratios, self-similar mean velocity profiles for different values of downstream location prevails up to the beginning of interaction region. The streamwise and lateral turbulence intensities increase with increasing the streamwise distance up to the interaction region, where the turbulence behavior becomes random and is characterized by larger peak values of the turbulence intensity compared to wall jet region. The maximum velocity decay and jet half-width growth increased parabolically with streamwise distance. No significant effect of conical shape was observed. Surface flow visualization was carried out for several exit jet velocity ratios. Three dimensionality was seen to be reduced as the secondary jet momentum increases.

Keywords: conical wall jets; merged jet; half-width growth; jet decay; Reynolds stress

Introduction

Extensive studies of wall jets have been carried out because of their numerous applications in aeronautics and heat transfer (Dakos et al. 1984). In aeronautical applications, wall jets are primarily used on jet flaps, boundary-layer control devices, and circulation control applications (Wood 1981). Detailed accounts of turbulent wall jets, their characteristics, and extensive literature review are found in the review paper of Launder and Rodi (1991).

Kind and Suthanthiran (1973) experimentally studied the interaction of two opposing plane turbulent wall jets in still air. The interaction occurs at a position such that the ratio of exit momentum fluxes equal to the ratio of the interaction position from the two slots, the free jet that results from the interaction acquires the same time average velocity distribution as a conventionally generated free jet.

Rew and Park (1988) produced an experimental study of the interaction of two opposing, asymmetric curved wall jets. An experimental investigation was made of a two-dimensional (2-D) flow formed by the interaction of two asymmetric turbulent curved wall jets past a circular cylinder in still air. It was shown that the location of the interaction point was found to depend on the ratio of momentum fluxes of the two wall jets. Collision of two wall jets resulted in a significant pressure rise in the interaction region. The measured pressure distributions for equal initial momentum flux were seen to be symmetric about the line of interaction. The velocity and turbulence intensity profiles of the merged jet were similar to those of the plane turbulent jets. Park and Rew (1991) produced turbulence measurements in a merged jet from two identical opposing curved wall jets issuing tangentially on a cylindrical surface.

The present work was motivated by the possible use of opposite wall jets to control the vortical flow over the forebody of fighter aircraft as a mean of controlling the side force due to flow asymmetry when operating at high angle of attack. These measurements are part of a wind-tunnel investigation to evaluate the effectiveness of controlling the symmetry of forebody vortices at high angle of attack. In the absence of free stream, these measurements are performed for validating a simplified boundary-layer-type analysis of the present conical flow model. The flow model in this case; i.e., in the absence of free stream, is 2-D to the first order of b/R. These measurements will be used to obtain a parameter taking into account the cross-flow free-stream Reynolds number and the required ratio of jet momentum fluxes to maintain a zero side force on the circular cone.

Experimental investigation of the flow field due to opposing conical wall jets past a slender circular cone before, during, and after the two jets merge into a single free jet was carried out. The two jets are issued tangentially to the cone surface from two

Address reprint requests to Dr. M. A. Jarrah, Department of Mechanical Engineering, Jordan University of Science and Technology, Irbid, Jordan.

Received 7 April 1994; accepted 11 November 1995

Int. J. Heat and Fluid Flow 17: 397–402, 1996

655 Avenue of the Americas, New York, NY 10010

0142-727X/96/$15.00
PII S0142-727X(95)00104-2

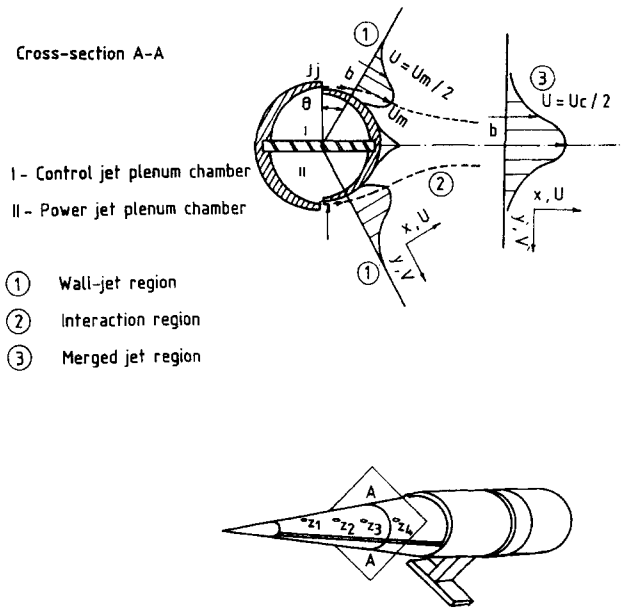

Figure 1 Experimental apparatus and flow configuration

opposing slots and develop initially as curved wall jets. After some distance along the surface, they collide and interact with each other in a region called the interaction region. The two jets then merge into a single free jet, which proceeds downstream away from the cone surface and is referred to as the merged jet. For an effective depiction of the opposing flow, it was convenient to identify the jets by their initial momentum flux. The wall jet with larger initial momentum flux or exit velocity was referred to as the power jet, and the one with the smaller momentum flux was called the control jet. The flow is sketched in Figure 1. Extensive flow-field survey was produced including surface flow visualization to help in understanding the resulting flow field, flow direction, and model end effects.

Experimental setup

A schematic of the experimental setup is shown in Figure 1. The setup is made of a circular cone consisting of two halfs. Apex angles of the upper and lower halves are 15 and 16°, respectively. This results in two conical slots with a constant slot height-to-radius of curvature ratio ($h/R = 0.0678$). This ratio plays a significant role in achieving two dimensionality. The present slot height-to-radius of curvature ratio is considered to form a mildly curved wall jet, (h/R less than 10%). The cone plenum is divided into two independent chambers. By adjusting the valves located at the inlet of each chamber, the desired ratio of control jet-to-power jet velocities was achieved. The power jet velocity was fixed at 30 m/s, and the control jet velocity was varied to obtain the desired ratio of momentum fluxes of the two jets.

Compressed air was supplied by a 7.5 hp reciprocating compressor at 7–10 bar. A pressure regulator was installed before the model to maintain the pressure at 5.7 bar to reduce compressor pulsation effects on the experiment. Measurements were made at four stations along the axis of the cone. These stations were marked by a Z position. These positions were selected to have a 30-mm separation along the axis of the cone. Measurements stations are shown in Figure 1.

Flow-field measurements were made by single and cross hot wires constant temperature anemometers. Standard probes made of 5-μm gold-plated tungsten wires were used with an overheat ratio set at 0.8 and the x-probe yaw angles of $\pm 45°$. Data acquisition was performed using a 12-bit A/D converter installed in an AT personal computer. Sampling rate was set at 3000 samples/s/channel. Data were collected in records at each measurement point. Each data record was chosen to have a 10-s period.

Flow orientation was surveyed using hot-wire probe, Pitot-static tube, and a probe with tufts at its tip. No axial flow can be detected from this survey. A pitot static tube connected to a micromanometer having 0.01-mm resolution showed no significant variation (less than 0.5%) when the yaw angle is in the range of $\pm 5°$ degrees with respect to the plane normal to the longitudinal axis of the cone.

From the above survey, two regions are identified. The first region is characterized by smooth flow conditions with a small amount of fluctuations. This region extends from the slot exit to some angular position depending on the flow condition set by the ratio of the momentum of the two jets. The second region is characterized by a large amount of fluctuation. This region is located at the interface between the two jets and is called the interaction region. The flow structure in the interaction region is complex. This region is characterized by a sudden growth of the wall jet half width. Flow direction is circulatory in a plane normal to the cone axis due to the formation of vortex type structure above the cone.

The cross hot wire was operated with its prongs parallel to the flow direction; i.e., parallel to the main flow direction. The technique attributable to Vagt (1979) is used to evaluate the turbulence quantities. The detailed description of the measurement and calibration procedures is given in Al-Shorman (1992).

Correction to the measured turbulence intensities of the order of ± 10% was found to be necessary assuming that $\overline{w'^2}$ is of the order of $\overline{u'^2}$. Similar error analyses are reported by Tsuji and

Notation

b	wall jet half width, L
h	jet slot height, L
R	streamwise radius of curvature, L
u, v	streamwise, normal component of velocity, L/T
U	mean streamwise velocity, L/T
U_j	jet exit velocity, L/T
U_m	maximum mean streamwise velocity at a given streamwise distance x, L/T.
V_c	exit velocity of control jet, L/T
V_p	exit velocity of power jet, L/T
$\overline{u'^2}$	time mean square of fluctuation U component, L/T^2
$\overline{v'^2}$	time mean square of fluctuation V component, L/T^2
$\overline{u'v'}$	turbulent shear stress, L/T^2
x, y	streamwise, normal coordinates along cone surface, L
Z	axial position along the cone axis, L

Greek

θ	angle measured from power jet exit, °
ρ	Density, M/L^3
τ	shear stress $= \mu \partial u/\partial y - \rho \overline{u'v'}$, F/L^2

Nagano (1989). Inaccuracy due to high turbulence level close to the interaction region was compensated for according to guidelines presented by Muller (1982). Measurements in the interaction region of both turbulence and mean flow properties were taken and reduced, as were those in the wall jet region. The spatial accuracy was increased by using a magnifying glass to position the hot wire at the surface. The spatial accuracy is guaranteed to be $\leq \pm 0.1$ mm combined with the resolution of the stepping motor used for traversing the hot wire. This accuracy is reduced in the case of the cross wire when used close to the wall due to two sources: first, a large velocity gradient near the wall; and second, the poor spatial resolution of the cross wire near the wall. Spatial accuracy in the case of cross wire is ± 0.4 mm. This spatial accuracy was verified by comparing mean velocity profiles obtained via single-wire measurements with those measured by the cross wire.

Results and discussion

Nature of the flow field

A schematic view of the present flow-field cross section is shown in Figure 1. The flow structure was investigated using tufts and surface oil flow visualization. Surface oil flow visualization pictures indicate that the flow structure at each cross section resembles that of a flow past a circular cylinder to some degree. Flow visualization pictures (such as that shown in Figure 2) show that flow separates from the surface at an angular positions depending on the ratio of the jet momentum fluxes. The first separation line is on the power jet side. The second separation line is located on the control jet side. The region between the two separation lines is characterized by a complicated flow field. Flow details in the interaction region; i.e., between the two separation lines indicate that a reattachment line may be formed in this region closer to the control jet separation line. Results of the flow visualization are summarized in Table 1, where θ_p and θ_c are separation line angles corresponding to both the power jet and the control jet and are measured from the power jet slot.

An important feature of this flow field is the slot end effects. Separation lines near the slot ends are curved, indicating earlier separation, and form a typical three dimensional (3-D) vortical flow separation. A striking feature is that, as the ratio of jet momentum fluxes approaches unity, flow visualization indicates that slot end effects are greatly reduced confining the end effects to a small region near the slot ends and resulting in a sharper oil flow features.

Figure 2 Sample of surface flow visualization at $V_c/V_p = 0.6$

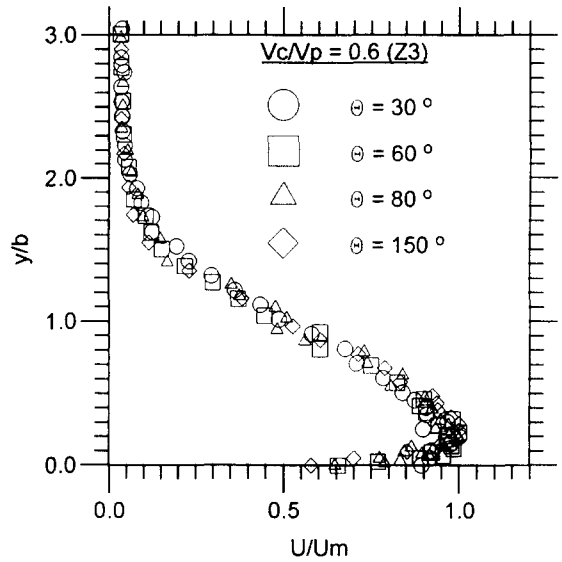

Figure 3 Self-similar mean velocity profiles in the conical wall-jet region

Mean flow and turbulence intensities in the wall jet region

Curved wall jets achieve self-similar mean velocity profiles if measurements were taken in the curved wall jet region; i.e, away from the interaction region, also if the velocity and distance from the wall are normalized by appropriate characteristic velocity scale and length scale, respectively. These characteristic scales are the local maximum velocity and the jet half width. The jet half width is defined as the distance from the wall to the location where the velocity is equal to half of the maximum velocity. Figure 1 defines the nomenclature for opposing curved wall jets. The angle θ measures the angular position of the measurements on the surface of the cone. In this experiment, the power jet and control jet slots are located at $\theta = 0°$ and $\theta = 180°$, respectively.

Mean velocity profiles in the wall jet region normalized by the maximum jet velocity *versus* y (distance measured from the surface in the radial direction) normalized by the half width are summarized for $V_c/V_p = 0.6$ in Figure 3 using single hot wire. The dimensionless velocity profiles seem to be self-similar, unaffected by the streamwise distance in curved wall jet regions. No appreciable discrepancies exist between the velocity profiles in the curved wall jet regions with different control to power jet velocities ratio V_c/V_p (Al-Sarkhi 1993).

The half-width growth in the curved wall jet region has a parabolic shape, shown in Figure 4. It is clear that it grows rapidly as the interaction region is approached. From this figure, we can identify the beginning and the end of the interaction region. The interaction region identified by the sudden growth of b/h is consistent with flow visualization results (see Figure 2). There is self-similar behavior of wall jet half-width growth with streamwise distance in the first wall jet region. Past the interaction region, the behavior returns to the parabolic shape in the next wall jet region on the other side of the cone. In other words, there

Table 1 Results of flow visualization

V_c/V_p	$\theta_p°$	$\theta_c°$
0.4	105	150
0.6	80	135
0.8	75	120
1.0	60	120

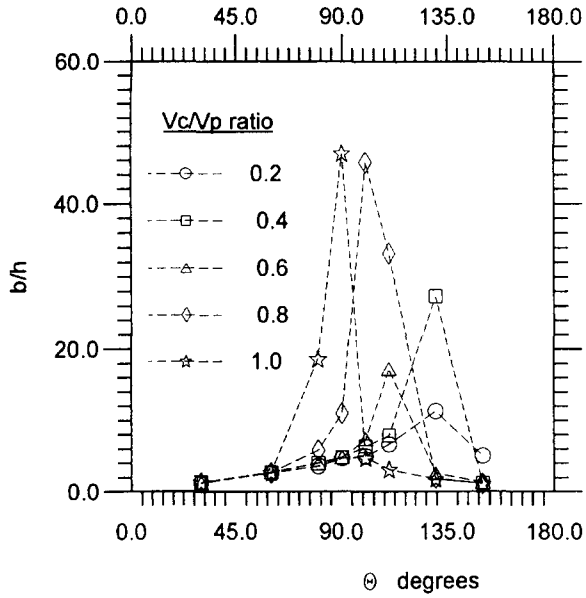

Figure 4 Half-width growth in the conical wall-jet and interaction regions

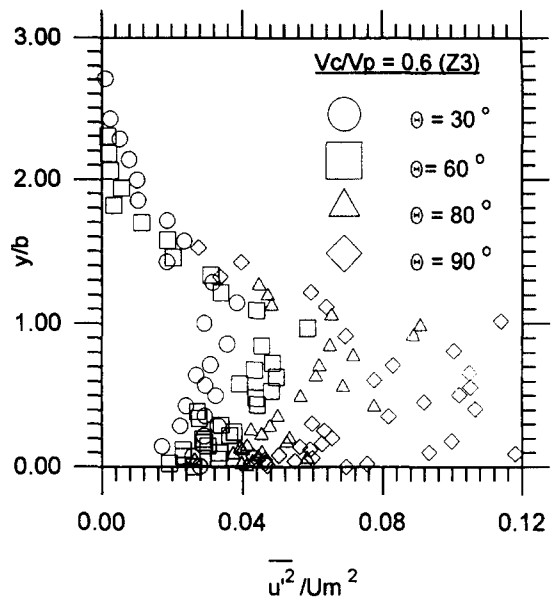

Figure 6 Streamwise normal stress profiles in the conical wall-jet region

is no effect of control-to-power velocity ratio (V_c/V_p) on the half-width growth (b/h), in the wall jet region; i.e., the wall jet is unaware of the second jet in the wall jet region. However, a strong effect is clearly observed in the interaction region as V_c/V_p increases, the growth rate increases, and interaction region moves from control jet side toward power jet side.

The maximum velocity decay displayed a parabolic shape in the wall jet region, as shown in Figure 5. The decay of the maximum velocity is close to the single jet case, i.e., zero V_c/V_p ratio up to the interaction region. The decay of maximum velocity at $V_c/V_p = 1$ is higher than that at $V_c/V_p = 0$ due to the increased growth of jet half width. The peak of both the half-width growth or maximum velocity decay is at the middle of the interaction region.

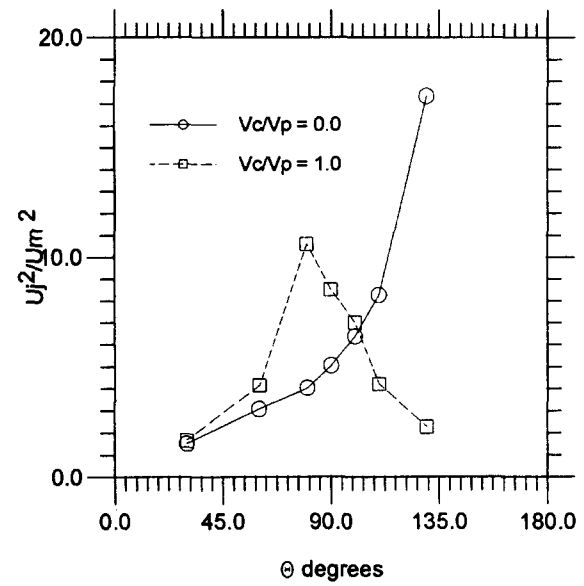

Figure 5 Maximum velocity decay in the conical wall-jet and interaction regions

Turbulent quantities in the conical wall jet and interaction region

The turbulence data for the curved conical wall jets are presented in Figures 6–10 for a sample case of $V_c/V_p = 0.6$. These results show that, although the mean velocity profiles were self-similar, the turbulence quantities were not. The degree of similarity in turbulent quantities increased far away from wall nearly at values of $y/b > 1.5$. In general, the lateral normal stress, $\overline{v'^2}/Um^2$ was more self-similar than the streamwise normal stress, $\overline{u'^2}/Um^2$ and the Reynolds shear stress, $\overline{u'v'}/Um^2$.

Streamwise normal stress, $\overline{u'^2}/Um^2$ affected strongly by the streamwise distance, and the peak value of $\overline{u'^2}/Um^2$ increases with increasing streamwise distance. Figure 6 shows that streamwise turbulence intensity peak is doubled for $\Theta = 80°$ compared with $\Theta = 60°$; i.e, the rate of growth becomes larger past the later position. This marked increase in $\overline{u'^2}/Um^2$ is attributed to the

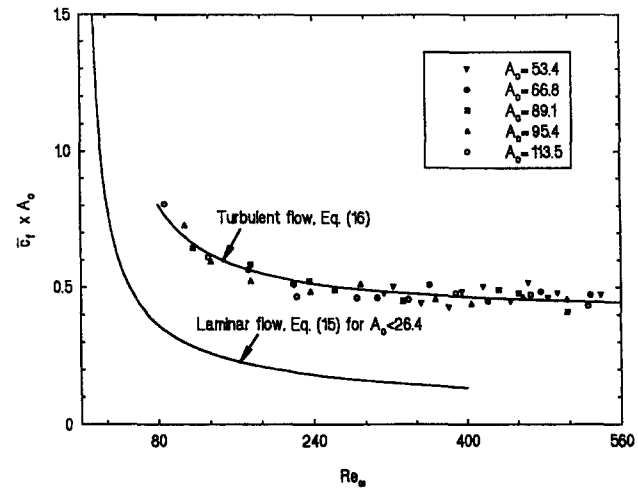

Figure 7 Lateral normal stress profiles in the conical wall-jet region

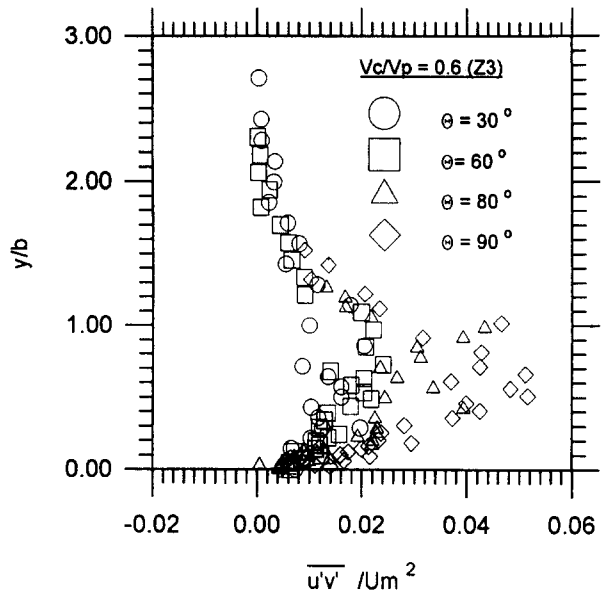

Figure 8 Shear stress profiles in the cconical wall-jet region

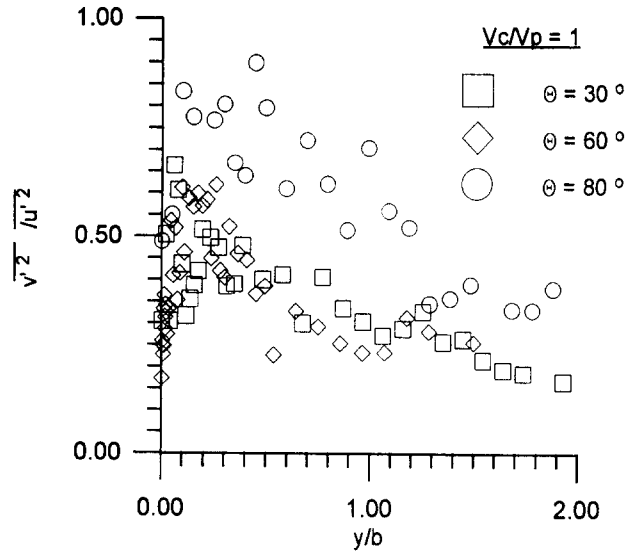

Figure 10 Ratio of streamwise and radial fluctuations

large increase in the adverse pressure gradient past $\Theta = 60°$ position. This conclusion is confirmed by Park and Rew (1991) in their measurements of two opposing curved wall jets. Lateral turbulence intensity experience less influence of the adverse pressure gradient, as shown by Figure 7. This is attributed to the damping mechanism of the wall to the lateral component of turbulence. Inner-layer shear stress crossover point was found to be located very close to the wall. Positive shear stress was obtained in shear stress profiles through the interaction region. Considering the spatial resolution of the measurements, this indicates that the thickness of the shear layer is reduced in conical wall jets. In the interaction region, both longitudinal and lateral turbulence intensities approach zero values at the wall. Turbulence intensities in the conical wall jet are higher than those obtained for 2-D curved wall jets reported by Park and Rew.

Figure 8 shows a shear stress profile for $V_c/V_p = 0.6$. A shear stress profile should start at positive value at the wall decrease and then become negative in the inner layer. In the present experiment, the shear stress profile starts at nearly zero value at the wall. This attributed to the thin wall jet and to the spatial resolution of the cross wire. In the interaction region; i.e., for large streamwise distance, a positive shear stress was measured.

Correlation coefficient for $V_c/V_p = 0.6$ at various streamwise locations is plotted in Figure 9. Correlation coefficient measures the local state of equilibrium of turbulent structure. The value of the correlation coefficient is about 0.55 for $\Theta = 30$ and 60°. For larger streamwise locations, its value is increased to about 0.7. This attributed to the large adverse pressure gradient in this region. Lower correlation coefficients are reported in the literature (Alcaraz et al. 1977). These results agree with those obtained by Park and Rew (1991). The ratio of $\overline{v'^2}/\overline{u'^2}$ is plotted at several streamwise locations for the case of $V_c/V_p = 0.6$ in Figure 10. This ratio is a measure of the coherence of turbulent eddies. The value for this parameter agrees well with Park and Rew results for the range of their measurements. However, values $\overline{v'^2}/\overline{u'^2}$ are larger as separation is approached; i.e., deep in the adverse pressure gradient region.

The degree of self-similarity of the normalized turbulent quantities decreases as the streamwise distance increases up to the interaction region. In this region, the turbulent fluctuations are very high, and the measurements are not expected to be accurate. The behavior of turbulent quantities becomes nearly random due to flow separation. The measured turbulent quantities in the interaction region are reported by Al-Sarkhi (1993). Although measurements of turbulent intensities is qualitative in this region, these measurements display some distinct features. The interaction region is marked by turbulence intensities characterized by a high rate of increase in the sublayer and a sharp maximum near the wall (at values of $y/b < 0.5$). This character of the turbulence intensities near the wall is similar to that obtained in turbulent boundary-layer separation.

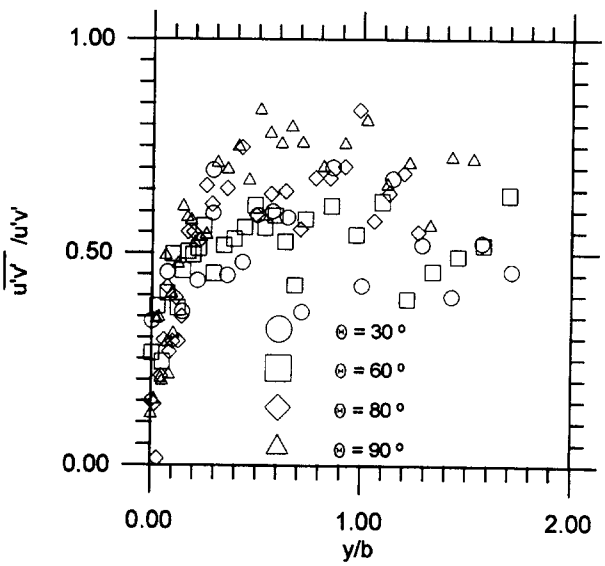

Figure 9 Correlation coefficients of the conical wall-jet

Merged jet region

In the merged jet region, the two wall jets coalesced into a single free jet that proceeds downstream away from the cone surface. The merged jet measurements were taken at $V_c/V_p = 1$ and $\theta = 90°$ using a single hot wire. This jet has a mean velocity profile similar to that of a conventional free jet. The mean velocity of the merged jet decreases with increasing the normalized distance from the centerline with the well-known bell shape.

After the two opposing wall jets separate and interact with each other, a single free jet emerges. If the power and control jets are identical, the merged jet will have its plane of symmetry normal to the cone surface at $\theta = 90°$, but when the power jet has larger momentum flux than the control jet, the merged jet will deflect toward the control jet side, this is supported by the flow visualization pictures (Figure 2). The normalized streamwise turbulence intensity, $\overline{u'^2}/Um^2$, profiles of the present study are in agreement with those of conventional free jets (see Al-Sarkhi 1993). More detailed measurements are needed to confirm the similarity between the merged jet region and the plane turbulent jet.

Conclusions

The interaction of two opposing curved wall jets developed over a conical surface was investigated experimentally. Flow-field measurements including mean flow and Reynolds stresses were performed; flow visualization was also carried out. The following conclusions may be drawn.

(1) The flow field was divided into three regions: the curved wall jet region, the interaction region; and the merged jet region. The location of interaction region was found to depend on the ratio of the two wall jets velocities (V_c/V_p). As (V_c/V_p) increases, the interaction region moves toward the power jet until it reaches the center of the upper surface of cone at $V_c/V_p = 1$.

(2) Test results indicate that flow properties are not affected by the conical geometry of the present model. Higher turbulence intensities, half-width growth, and maximum velocity decay were recorded as the slot ends were approached. This is attributed to slot end effects.

(3) The maximum velocity decay and half-width growth increase parabolically in curved wall jet region followed by a sharp increase of the maximum velocity decay and half-width growth in the interaction region.

(4) Although, self-similar mean velocity profiles were obtained in the wall jet region, the resulting turbulence intensities were not self-similar; i.e., the resulting flow is not self-similar.

(5) There is no significant effect of increasing control jet on flow field through the wall jet region. However, strong effects appear in the interaction region. The effect in the interaction region is multidimensional. Increasing V_c/V_p confines the slot end effects to a smaller region, turbulent intensities are larger with a sharper peak closer to the wall.

References

Alcaraz, E., Charnay, G. and Mathieu, J. 1977. Measurements in a wall jet over a convex surface. *Phys. Fluids*, **20**, 203–210

Al-Sarkhi A. S. 1993. Interaction of conical wall jets. M.Sc. thesis, Department of Mechanical Engineering, Jordan University of Science and Technology, Irbid, Jordan

Al-Shorman, A. 1992. Interaction of conical wall jet over a conical body of revolution. M.Sc. thesis, Department of Mechanical Engineering, Jordan University of Science and Technology, Irbid, Jordan

Dakos, T., Verriopoulos, C. A. and Gibson, M. 1984. Turbulent flow with heat transfer in plane and curved wall-jets. *J. Fluid Mech.*, **145**, 339–360

Kind, R. and Suthanthiran, K. 1973. The interaction of opposing plane turbulent wall jets. *J. Fluid Mech.*, **58**, 389–402

Launder, B. E. and Rodi, W. 1981. The turbulent wall jet. *Prog. Aerospace Sci.*, **19**, 81–128

Muller, U. R. 1982. On the accuracy of turbulence measurements with inclined hot wires. *J. Fluid Mech.*, **119**, 155–172

Park, S. and Rew, H. 1991. Turbulent measurements in a merged jets from two opposing curved wall jets. *Exp. Fluids*, **10**, 241–250

Rew, H. and Park, S. 1988. The interaction of two opposing asymmetric curved jets. *Exp. Fluids*, **6**, 243–252

Tsuji, T. and Nagano, Y. 1989. An anemometry technique for turbulence measurements at low velocities. *Exp. Fluids*, **7**, 547–559

Vagt, J. 1979. Hot wire probes in low speed flow. *Prog. Aerospace Sci.*, **18**, 271–323

Wood, N. J. 1981. The aerodynamics of circulation control airfoils. JIAA TR-41 Dept. of Aero/Astro, Stanford University, Stanford, CA